

BARKHAUSEN DEMODULATION

B. R. Ortquist
D. T. Hayford
Engineering Physics Group
Battelle Memorial Institute
505 King Avenue
Columbus, OH 43201

INTRODUCTION

A careful examination of the magnetization of a ferromagnetic material reveals that it is a discontinuous process; when subject to a varying magnetic field, a ferromagnetic material is magnetized in discrete bursts as domain boundaries overcome pinning at defects in the crystal lattice. This discrete behavior manifests itself as high frequency "noise" superimposed upon a measurement of magnetic flux and is commonly referred to as the Barkhausen Effect. Several important microstructural properties of steel also depend on lattice defect structure, *i.e.*, mechanical hardness, ferrite content, material fatigue, and internal stress state, and investigators have successfully correlated Barkhausen Effect parameters with these properties [1-3]. Unfortunately, Barkhausen noise signals are broadband and weak, characteristics that often limit the utility of the Barkhausen Effect in NDE applications. In this paper, we will describe a phenomenon we call Barkhausen Demodulation, which provides a means of measuring Barkhausen noise that lends itself more readily to NDE investigations. Further, we will describe an experiment in which Barkhausen Demodulation was used to measure the hardness of X40 grade pipeline steel.

BACKGROUND

In the mid 1800s, an intellectually eclectic dentist by the name of Mahlon Loomis discovered that an amplitude modulated, high frequency electromagnetic field can be demodulated using a ferromagnetic pickup subject to a slowly varying magnetic field [4]. From this observation, he was able to develop a receiver capable of demodulating amplitude-modulated RF radiation, and subsequently, to demonstrate the world's first wireless telegraphy device. For this invention, Loomis was granted a patent in 1872. The phenomenon that he exploited, sometimes called the Loomis Effect, could not be explained in his day - it would depend on Barkhausen's discovery of his eponymous effect circa 1918. What follows is a qualitative explanation of the Loomis Effect, which we have chosen to call by the more descriptive name of Barkhausen Demodulation. First, however, a brief discussion of the mechanisms of magnetic domain growth and the Barkhausen Effect is in order.

THE BARKHAUSEN EFFECT

The dynamics of magnetic domain growth is largely responsible for the colorful magnetic behavior - hysteresis, the Barkhausen Effect, and other non-linear phenomena - exhibited by a ferromagnetic material under the influence of a magnetic field. Domain growth can be classified into three types: reversible domain wall displacements, irreversible domain wall displacements, and reversible domain rotations. Reversible domain wall displacements occur for an initially unmagnetized sample subjected to a small magnetic field. In this type of domain growth, domain wall motions proceed unimpeded such that domains oriented in the direction of easy magnetization nearest to that of the applied field (favorably aligned domains) are increased in size while domains of other orientations remain unchanged or are decreased in size. Because the domain motions are unimpeded, a cyclical change in field will cause no net change in magnetization, thus this type of domain growth is reversible.

Irreversible domain wall displacements occur for intermediate applied fields (and for small fields when the sample is magnetized). In this type of domain growth, domain wall motions proceed unimpeded until domain walls become pinned at impurities or discontinuities in the crystal lattice. As the applied field is further increased in magnitude, pinned domain walls eventually acquire enough energy to overcome pinning and domain growth resumes until the next pinning sites are encountered. As a result, domain growth occurs in bursts as favorably aligned domains increase in size and those unfavorably aligned remain unchanged or decrease in size following each pinning break. This discrete character of the magnetization is known as the Barkhausen Effect and each pinning break is called a Barkhausen Event. Because of the quantized character of the Barkhausen Events, a cyclical change in field will not, in general, leave the magnetization unchanged, thus this type of domain growth is irreversible.

Reversible domain rotations occur for large applied fields after favorably aligned domains have grown to the limits imposed by crystalline boundaries. In this type of domain growth (though, here, "growth" is a misnomer), the magnetization of the sample increases in the direction of the applied field as the individual dipole moments comprising favorably aligned domains rotate into this direction. If the magnitude of the applied field is subsequently reduced, the dipole moments will rotate back into the domain direction (the most favorably aligned direction of easy magnetization), thus, this type of domain growth is reversible.

Figure 1 shows a typical magnetization curve for a ferromagnetic material. Regions of the curve in which each of the three types of domain growth dominate are marked on the figure. Also, a portion of the curve lying in the region dominated by irreversible domain wall displacements has been blown up to illustrate the discrete nature of magnetization associated with the Barkhausen Effect.

BARKHAUSEN DEMODULATION

For the following discussion, we will adopt a very simple model of an iron-based material that is useful for illustrating domain growth when the material is subject to an external magnetic field. Figure 2a depicts the model, in which four of the easy directions of magnetization are considered, denoted $\pm y$ and $\pm z$, with one domain oriented in each direction (ferritic steel has a cubic crystal structure and, thus, in reality, has six easy directions). A pinning site has been located at the point of intersection of the domain walls. Though this is a simplistic model, the arguments that follow can easily be generalized beyond these assumptions.

If the specimen is subjected to a slowly increasing magnetic field in the $+z$ direction, H_z , domains oriented in this direction will grow at the expense of domains less favorably oriented, especially those oriented in the $-z$ direction. Domain growth will continue in this manner until domain walls become pinned. Figure 2b shows the domain wall displacements resulting from the application of H_z . As indicated in the figure, domain walls A and D shift such that the $+z$ domain increases in size, while the movements of domain walls B and C cause the $-z$ domain to decrease in size. The sizes of the $+y$ and $-y$ domains remain roughly unchanged.

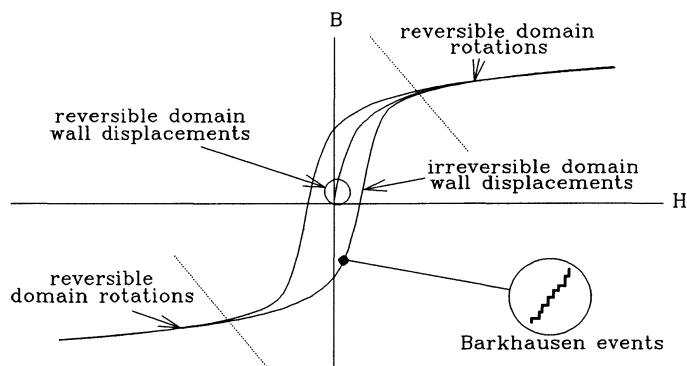


Figure 1. Magnetization curve for a ferromagnetic material. The curve is divided into regions according to the dominant form of domain growth occurring in each region. A portion of the curve is blown up to indicate the discrete character of magnetization associated with the Barkhausen Effect.

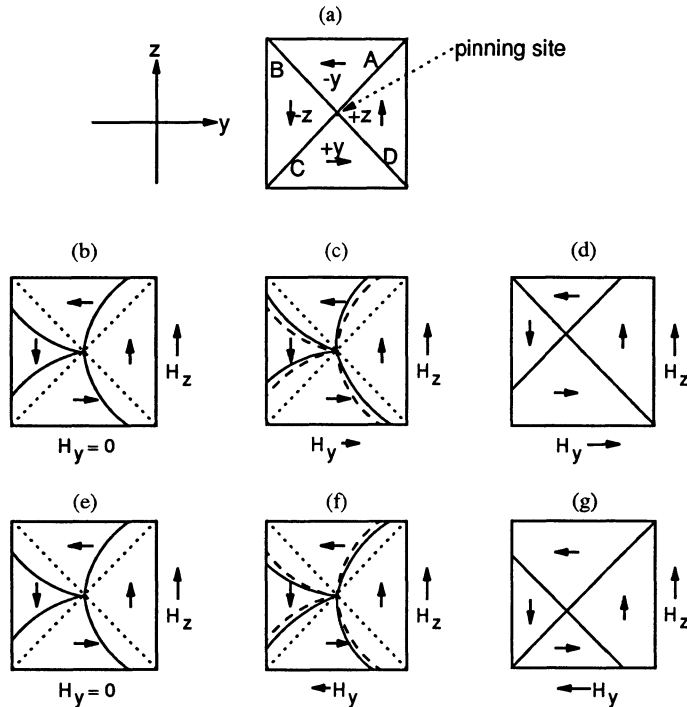


Figure 2. a. Pictorial magnetic domain model illustrating absolute value effect. Domain orientations are indicated by arrows and domain walls separating domains are labeled A-D. A pinning site is located at the intersection of the four domains. b. Domain wall displacements (solid lines) resulting from the application of H_z . c. Domain wall displacements resulting from the application of H_y oriented in the $+y$ direction. The dashed lines indicate the previous domain wall positions. d. Resulting domain sizes after walls A and C overcome pinning showing that the $+z$ domain has grown. e. Same as (b). f. Domain wall displacements resulting from the application of H_y oriented in the $-y$ direction. g. Resulting domain sizes after walls B and D overcome pinning showing that the $+z$ domain has again grown.

If, in addition to H_z , a high frequency, low amplitude AC field is added along the y axis, the resulting domain wall displacements tend to oppose certain displacements caused by H_z and enforce others. Here, two cases must be considered, corresponding to the two orientations of H_y . First, when H_y points in the $+y$ direction, domain walls A and C are further stressed whereas domain walls B and D are relaxed slightly. This situation is depicted in Figure 2c where the dashed lines represent the former domain wall positions. Ultimately, the additional energy imparted to domain walls A and C by H_y will be sufficient to break the pinning of these walls. At the same time, the slight reduction of energy of domain walls B and D will prevent these walls from overcoming pinning. The net result is that the $+z$ and $+y$ domains increase in size at the expense of the $-z$ and $-y$ domains (Figure 2d).

In the second case, H_y points in the $-y$ direction. As indicated in Figure 2f, it is the motions of domain walls B and D that are augmented by H_y and those of domain walls A and C that are opposed. Hence, in this case, it is domain walls B and D that overcome pinning, and domain walls A and C that do not. Accordingly, the $+z$ and $-y$ domains grow, while the $-z$ and $+y$ domains are depleted (Figure 2g).

In summary, regardless of the orientation of H_y , the magnetization of the sample increases in the $+z$ direction. The steel sample acts as a circuit element that transforms an oscillating input signal (H_y) into its absolute value (times some constant). Figure 3a is a plot of representative input and output waveforms clearly showing the absolute value effect. It is this nonlinear behavior that Loomis exploited to demodulate amplitude-modulated RF radiation. We will use the same effect to measure an output signal that is proportional to the number of Barkhausen events.

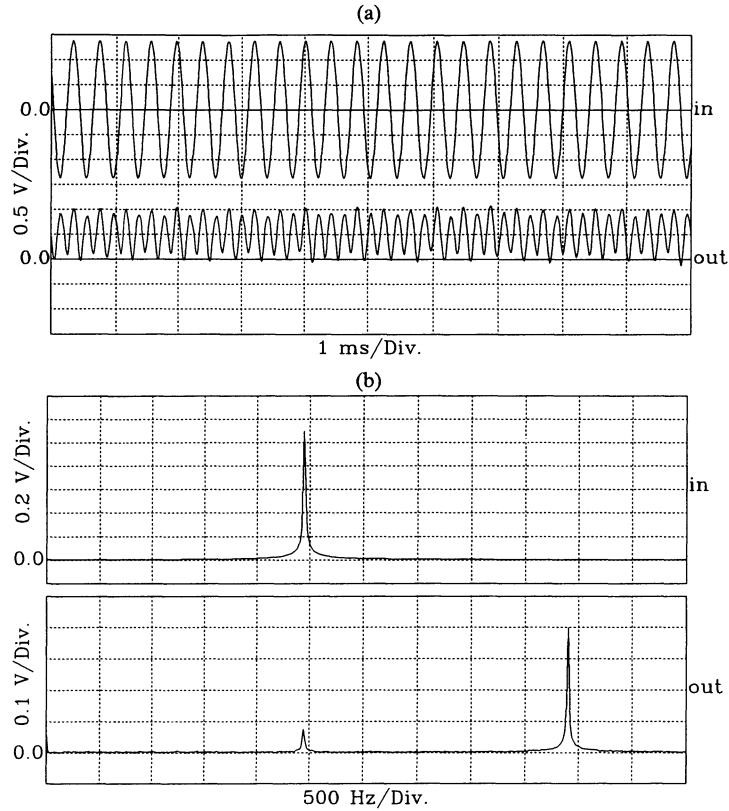


Figure 3. a. Sinewave input waveform and resulting output waveform demonstrating the absolute value effect. b. Spectra corresponding to the waveforms shown in (a).

MEASUREMENT TECHNIQUES

Figure 4 is a schematic of the basic experimental configuration used to measure Barkhausen noise amplitudes according to the principles discussed above. The setup consists of two electromagnets oriented transversely for magnetizing the sample along the y and z axes, respectively, a magnetometer placed near the sample in the vicinity of the y magnet and oriented in the +z direction, oscillators for driving the electromagnets, and a lock-in amplifier for observing the output of the magnetometer.

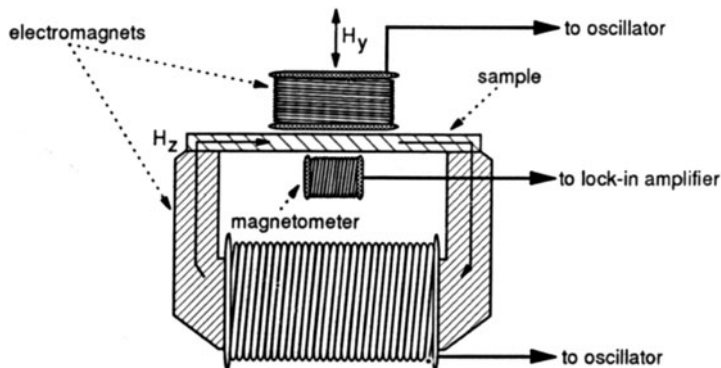


Figure 4. Experimental setup used to measure Barkhausen Demodulation.

There are two techniques for measuring Barkhausen noise using this setup. The most straightforward technique is to magnetize the sample with a slowly varying AC field using the z magnet and a lower amplitude, high frequency AC field with the y magnet. According to the discussion above, the output of the magnetometer at twice the frequency of the y field should then be proportional to the Barkhausen noise amplitude. Figure 3 shows representative input and output waveforms and corresponding spectra obtained using this technique. As expected, the output of the magnetometer falls primarily at twice the y field frequency. The small amplitude component at the y field frequency results from the slight coupling of the y magnet and the magnetometer. This points out a potential drawback of this approach. Because it is impossible to perfectly decouple the y magnet and the magnetometer spatially, any second harmonic in the y field (caused by an overdriven amplifier, perhaps, or an imperfect oscillator) will interfere with the desired signal.

The second and preferred technique exploits the Barkhausen Demodulation phenomenon. Since it is not feasible to spatially decouple the y magnet and the magnetometer, it is necessary to decouple them in frequency. This is accomplished by energizing the y magnet with a modulated AC signal and taking advantage of the demodulation effect. The y field has the form:

$$\begin{aligned} H_y &= A\left\{1 - \frac{\alpha}{2} + \frac{\alpha}{2}\sin(\omega_m t)\right\}\sin(\omega_c t) \\ &= A\left(1 - \frac{\alpha}{2}\right)\sin(\omega_c t) + \frac{A\alpha}{4}\left\{\cos[(\omega_c - \omega_m)t] - \cos[(\omega_c + \omega_m)t]\right\} \end{aligned} \quad (1)$$

where ω_c is the carrier frequency, ω_m is the modulation frequency, α is the modulation fraction ($0 \leq \alpha \leq 1$), and A is a constant. Note that the y field has no component at the modulation frequency. The output of the magnetometer is written:

$$V_o = k_z H_z + k_y |H_y| \quad (2)$$

where H_z is the amplitude of the z field. The constant k_z (k_y) describes the coupling between H_z (H_y), the sample, and the magnetometer. In addition, k_y depends on the number of Barkhausen events and their relative amplitudes, thus k_y is the quantity of interest. Henceforth, the very slow variation in H_z will be ignored. Since V_o is even in H_y , it can be expanded as a series in even powers of $k_y H_y$:

$$V_o = a_0 + a_2 k_y^2 H_y^2 + a_4 k_y^4 H_y^4 + \dots \quad (3)$$

where the a's are constants. After some algebraic manipulation, the second order term of this expression can be written:

$$\begin{aligned} a_2 k_y^2 H_y^2 &= a_2 A^2 k_y^2 \left\{ \frac{3}{16} + \frac{\sin(\omega_m t)}{4} - \frac{\sin[(2\omega_c + \omega_m)t]}{8} + \frac{\sin[(2\omega_c - \omega_m)t]}{8} \right. \\ &\quad \left. - \frac{3\cos(2\omega_c t)}{16} - \frac{\cos(2\omega_m t)}{16} + \frac{\cos[(2\omega_c + 2\omega_m)t]}{32} + \frac{\cos[(2\omega_c - 2\omega_m)t]}{32} \right\} \end{aligned} \quad (4)$$

where, for simplicity, α has been set to one, corresponding to 100% modulation. Thus, V_o has a component at the modulation frequency, components at the second harmonics of the modulation and carrier frequencies, and components at the sum and difference frequencies of twice the carrier frequency and the modulation frequency. Higher order terms in Equation 3 will add components at the modulation frequency, higher order even harmonics of the modulation and carrier frequencies, and combinations of the harmonics of the carrier and modulation frequencies. In this form, the demodulation effect is obvious; the output of the magnetometer at the modulation frequency is a function of the Barkhausen noise amplitude. Furthermore, unless the modulation frequency is a precise multiple of the carrier frequency, there will be no harmonic interference with the desired signal (even if the modulation frequency is a multiple of the carrier frequency, the harmonic interference will be negligible if the carrier frequency is sufficiently larger than the modulation frequency).

Figure 5 shows typical input and output waveforms and spectra obtained using this technique. As expected, the output signal falls primarily at the modulation frequency. The small frequency components near the carrier frequency are combinations of the carrier frequency and harmonics of the modulation frequency (including the fundamental) that result from the imperfect spatial decoupling of the y magnet and the magnetometer.

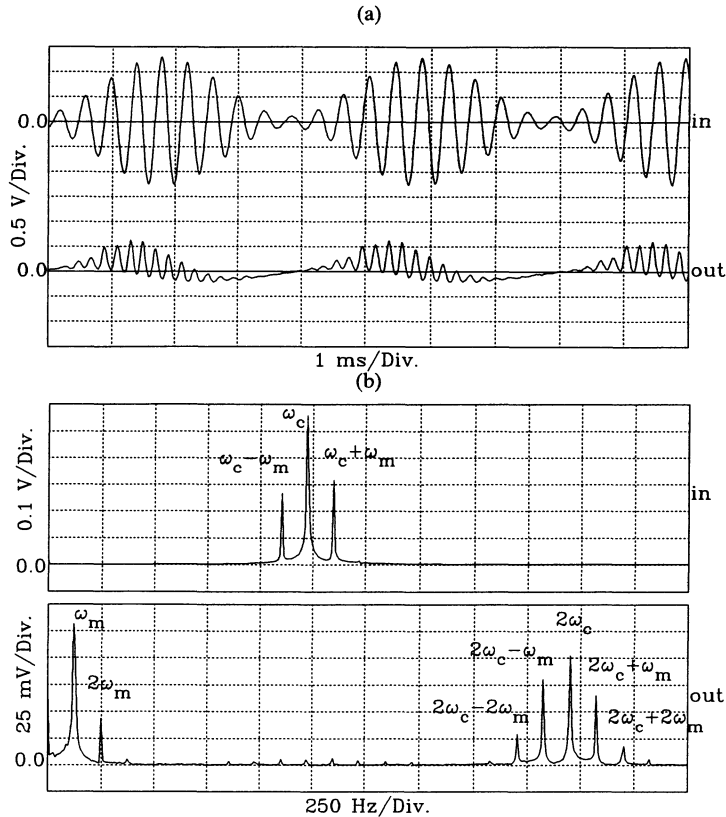


Figure 5. a. Modulated sinewave input waveform and resulting output waveform demonstrating the absolute value effect. b. Spectra corresponding to the waveforms shown in (a) demonstrating the demodulation effect.

APPLICATION

To demonstrate the potential utility of Barkhausen Demodulation in NDE applications, we used the method to measure the hardness of X40 grade pipeline steel.

Past investigators have successfully correlated hardness with magnetic coercivity for certain steels [2, 3]. Furthermore, it has been demonstrated experimentally that the maximum Barkhausen noise occurs for an external magnetic field strength, H , that is near the magnetic coercivity, H_C [3]. These data prompted us to search for a correlation between hardness and the H value for which the Barkhausen Demodulation signal was maximized. We will denote this value of the magnetic field H_B .

The experimental setup is shown in Figure 4. Additionally, a small coil was wrapped around each sample at its center and a Hall element was placed near this coil. These sensors were used to measure B along the sample axis and the axial component of H at the sample surface, respectively (B was recorded in order that we might determine H_C). The sample set consisted of 12 steel coupons of approximate dimensions $9 \times 0.5 \times 0.4$ ". The samples were heat treated to produce hardnesses ranging from 148 to 441 Brinell. The data were taken in the manner described in the second measurement technique above. Specifically, H_x was a 0.1 Hz triangle wave of sufficient amplitude to saturate the samples and H_y was a 10 kHz sinusoid 99.5 percent amplitude modulated at a frequency of 1 kHz and of amplitude ~ 1000 times less than H_x .

Each sample was completely demagnetized and then subjected to H_x and H_y , which varied in the manner described above. The magnetometer output at the modulation frequency (the Barkhausen amplitude) was recorded through 1-1/2 cycles of H_x , corresponding to a full magnetization curve. At the

same time, the outputs of the B field coil and the Hall element were recorded. Thus it was possible to determine both H_B and H_C for each sample.

Figures 6a and 6b are magnetization curves and Barkhausen Amplitudes corresponding to a "soft" sample and a "hard" sample, respectively. Clearly, both H_C and H_B are greater for the harder sample. In fact, as indicated in Figure 7a, a reasonably good correlation was observed between hardness and magnetic coercivity. Furthermore, Figure 6 demonstrates that H_B does correspond fairly closely to H_C . Figure 7b shows the relationship between H_B and H_C across the sample set. Although the slope is not unity, the relationship is linear, indicating that H_B can be used to determine H_C . This is an important feature of the technique for it provides a means of obtaining the magnetic coercivity without knowledge of B, which is difficult to measure in NDE applications. Finally, a good correlation was observed between hardness and H_B as shown in Figure 7c.

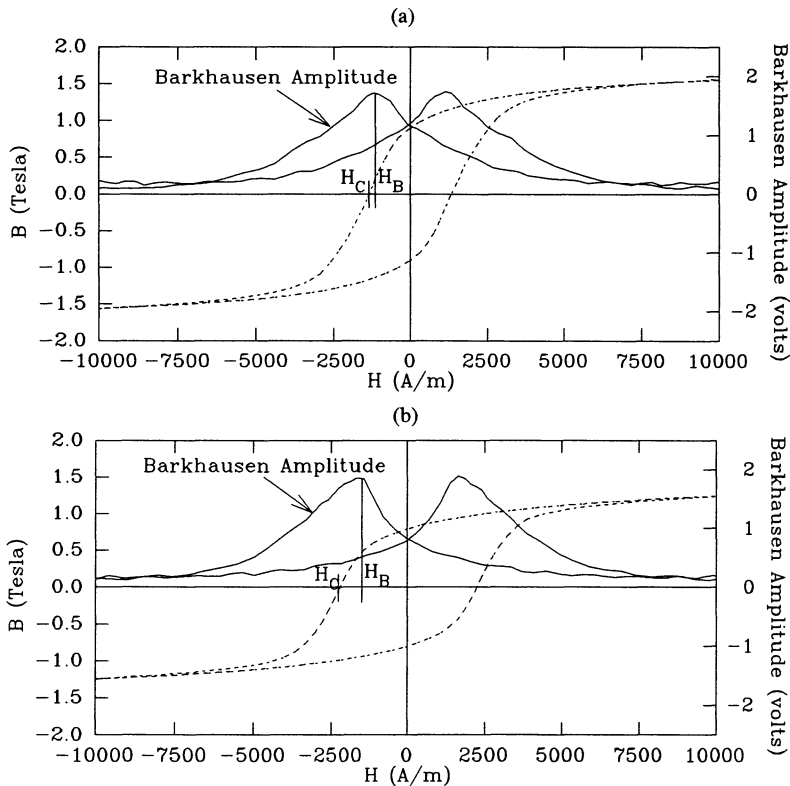


Figure 6. Magnetization curves and Barkhausen Amplitudes as a function of applied magnetic field for X40 grade pipeline steel samples. a. "Soft" sample. b. "Hard" sample.

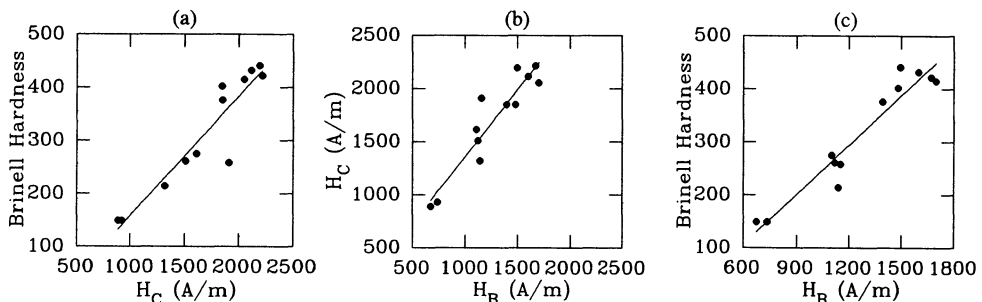


Figure 7. Experimental results for X40 grade pipeline steel: a. Brinell Hardness as a function H_C . b. H_C as a function of H_B . c. Brinell Hardness as a function of H_B .

CONCLUSIONS

Barkhausen Demodulation provides a technique of measuring Barkhausen noise that is easier to use in certain applications than conventional measurement techniques. The primary advantage of this technique over conventional techniques is that it converts the broadband Barkhausen noise signal into a proportional signal at a single frequency, thus admitting the use of synchronous detection techniques. Furthermore, the demodulation feature effects a complete decoupling of exciting and receiving coils, which is often difficult to achieve in conventional techniques.

We believe Barkhausen Demodulation can be used to advantage in NDE applications that currently rely on conventional techniques. As an example, we have demonstrated the use of Barkhausen Demodulation to measure the magnetic coercivity and mechanical hardness of X40 grade pipeline steel.

ACKNOWLEDGEMENTS

We thank Dr. James Corum for introducing us to the Loomis Effect and Mr. Milt Seiler for assisting in some of the experimental measurements of Barkhausen Demodulation.

REFERENCES

1. G. Matzkanin, R. Beissner, and C. Teller, *The Barkhausen Effect and its Applications to Nondestructive Evaluation*, SWRI - NTIAC Report 79-2.
2. B. Lavrent'ev, *Magnetic Structurescope Based on the Barkhausen Effect for Testing the Hardness of Heat-Treated Steel*, Soviet Journal of Nondestructive Testing, V. 20, No. 3 (1984).
3. W. Theiner and I. Altpeter, *Determination of Residual Stresses Using Micromagnetic Parameters*, New Procedures in Nondestructive Testing (Ed. P. Holler), Springer-Verlag, New York (1983).
4. J.F. Corum *et. al.*, *Dr. Mahlon Loomis: Terra Alta's Neglected Discoverer of RF Communication*, Proceedings of the Fifth International Tesla Symposium, Colorado Springs, Co. (1992).